Journal of Geophysical Research: Solid Earth

Supporting Information for

Sedimentary structure derived from multi-mode ambient noise tomography with dense OBS network at the Japan Trench

Lina Yamaya[1], Kimihiro Mochizuki[1], Takeshi Akuhara[1], Kiwamu Nishida[1]

[1]Earthquake Research Institute, The University of Tokyo, Bunkyo-ku, Tokyo, Japan

Contents of this file

Introduction

This supporting information provides six figures which are referred to as Figure S1–S10 in the article. The effect of the seafloor depth on the dispersion curves is shown in Figure S1. 1-D S-velocity structure inversion discarding the data of higher frequencies than 0.25 Hz is given in Figure S2. Grid points for inverting 2-D phase-velocity maps is given in Figure S3. Trade-off curves between RMS misfit and model variance for determining the damping parameters are given in Figure S4. Standard deviations for 2-D phase-velocity structures calculated by the bootstrap method are given in Figure S5. Checkerboard tests for phase velocity distributions are given in Figure S6 and S7. An example of the local 1-D non-liner inversion to estimate 3-D structure is shown in Figure S8. 3-D S-wave velocity structure inferred from different initial models are given in Figure S9. Sensitivity kernels of S-wave velocities for 1-D reference structure are given in Figure S10.

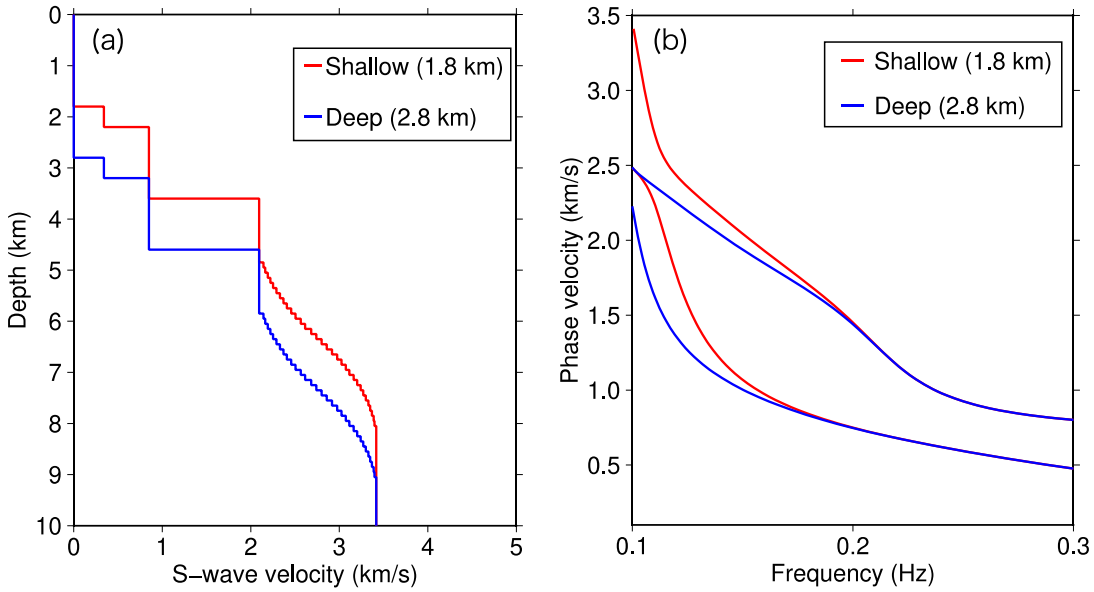

Figure S1. Difference of the dispersion curves depends on the seafloor depth. (a) S-wave velocity structure when the seafloor is shallowest (1.8 km depth) and deepest (2.8 km depth). (b) Phase-velocity dispersion curves for shallowest and deepest region. Both the fundamental and the first-higher mode are influenced at lower frequency (–0.2 Hz).

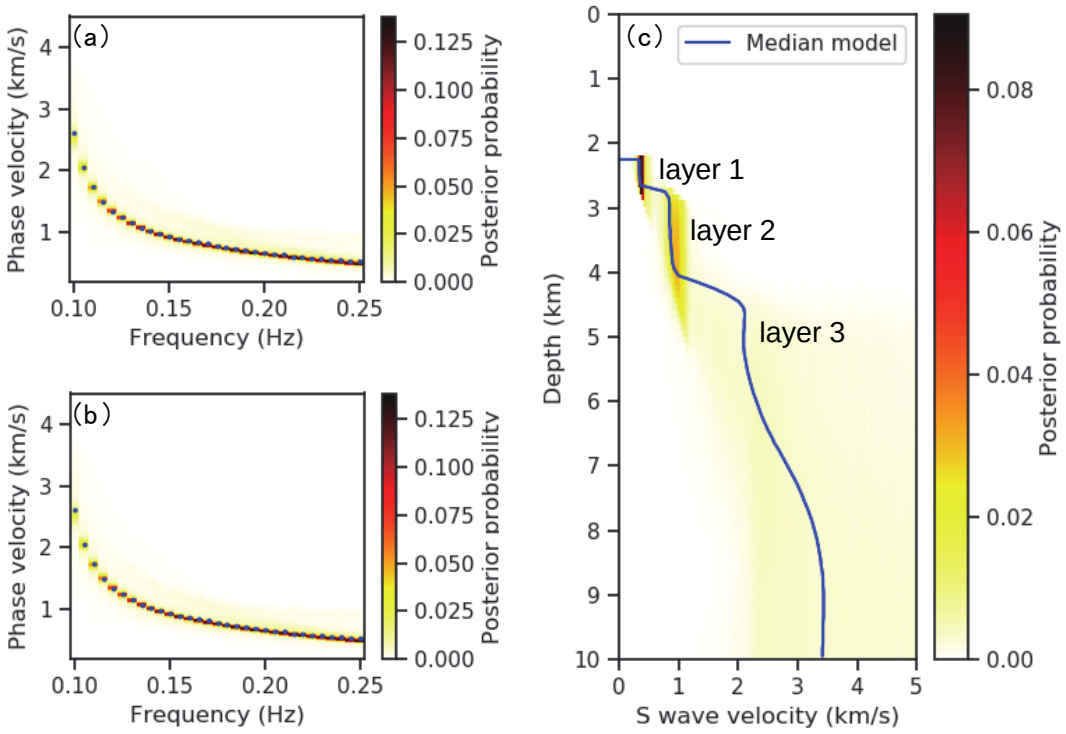

Figure S2. 1-D S-velocity structure inversion discarding the data of higher frequencies than 0.25 Hz, which showed low variance reductions in Figure 4d. (a) Phase velocity of the fundamental mode of Rayleigh wave. Blue points show the average phase velocities. The posterior probabilities were calculated for 1-D average S-wave velocity structures using the MCMC method. (b) Phase velocity of the first-higher mode of Rayleigh wave. Blue points show the 1-D average phase velocities. (c) S-wave velocity structure inferred by the MCMC method. The blue line shows the median velocity at each 0.1 km depth grid point.

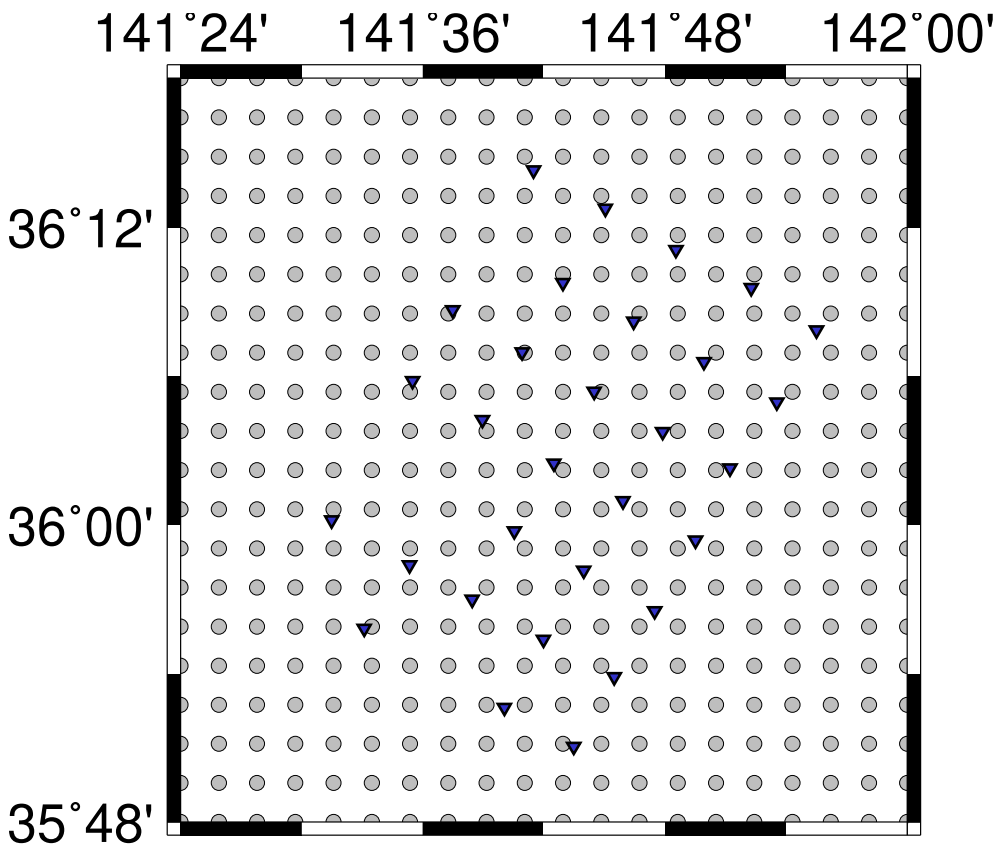

Figure S3. Grid points for inverting 2-D phase-velocity maps. The grey circles show the grid points. The grid intervals are 0.032° in longitude direction and 0.026° in latitude direction. Blue triangles show stations.

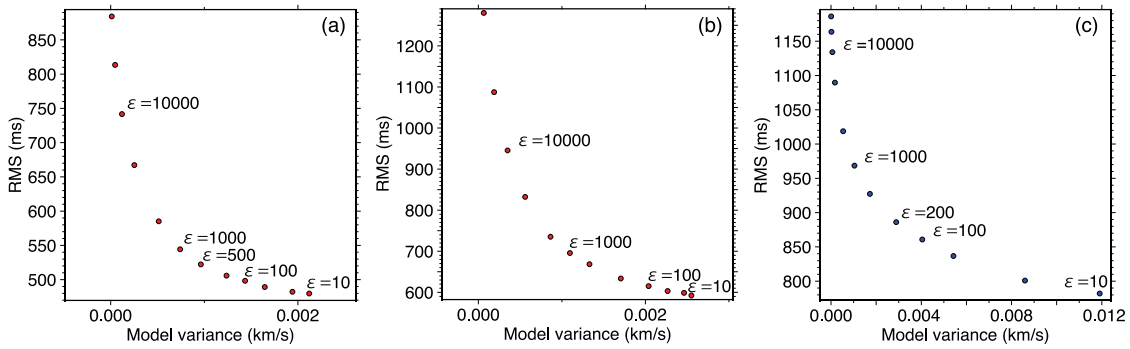

Figure S4. Trade-off curves between RMS misfit and model variance. (a) Fundamental mode at 0.15 Hz; ϵ = 500 is selected. (b) Fundamental mode at 0.2 Hz; ϵ = 1,000 is selected. (c) First-higher mode at 0.2 Hz; ϵ = 200 is selected.

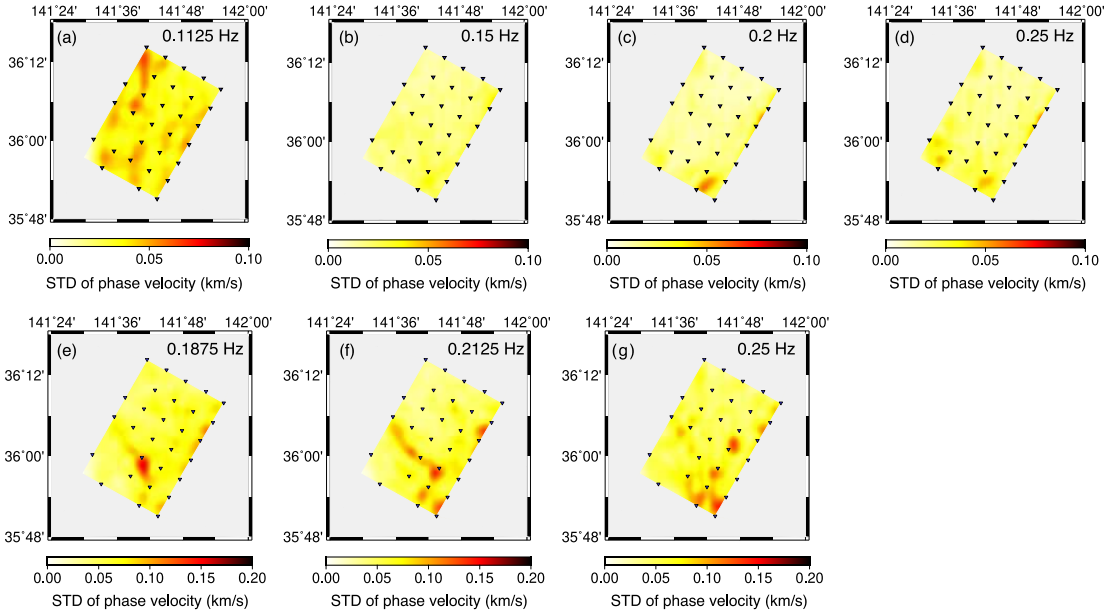

Figure S5. Standard deviations of phase velocities calculated by the bootstrap method for the fundamental mode of Rayleigh wave using the vertical components (a – d), and for the first-higher mode of Rayleigh wave using the radial components (e – g).

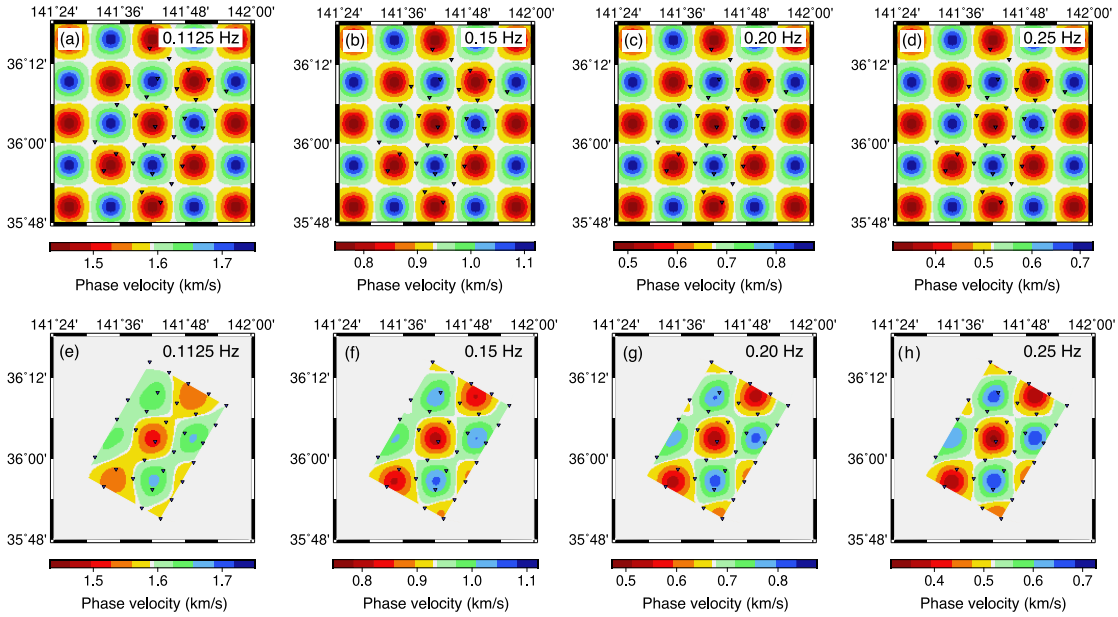

Figure S6. Checkerboard test for phase velocity distribution. (a – d) Input models for the fundamental mode of Rayleigh wave using the vertical components. (e – h) Resulted models. (a, e) Input and resulted models using phase velocities of each path obtained at 0.1125 Hz. (b, f) Models using data obtained at 0.15 Hz. (c, g) Models using data obtained at 0.2 Hz. (d, h) Models using data obtained at 0.25 Hz. The resolution depends on the frequency mainly because the obtained number of station pairs are different due to the quality of the cross spectrum.

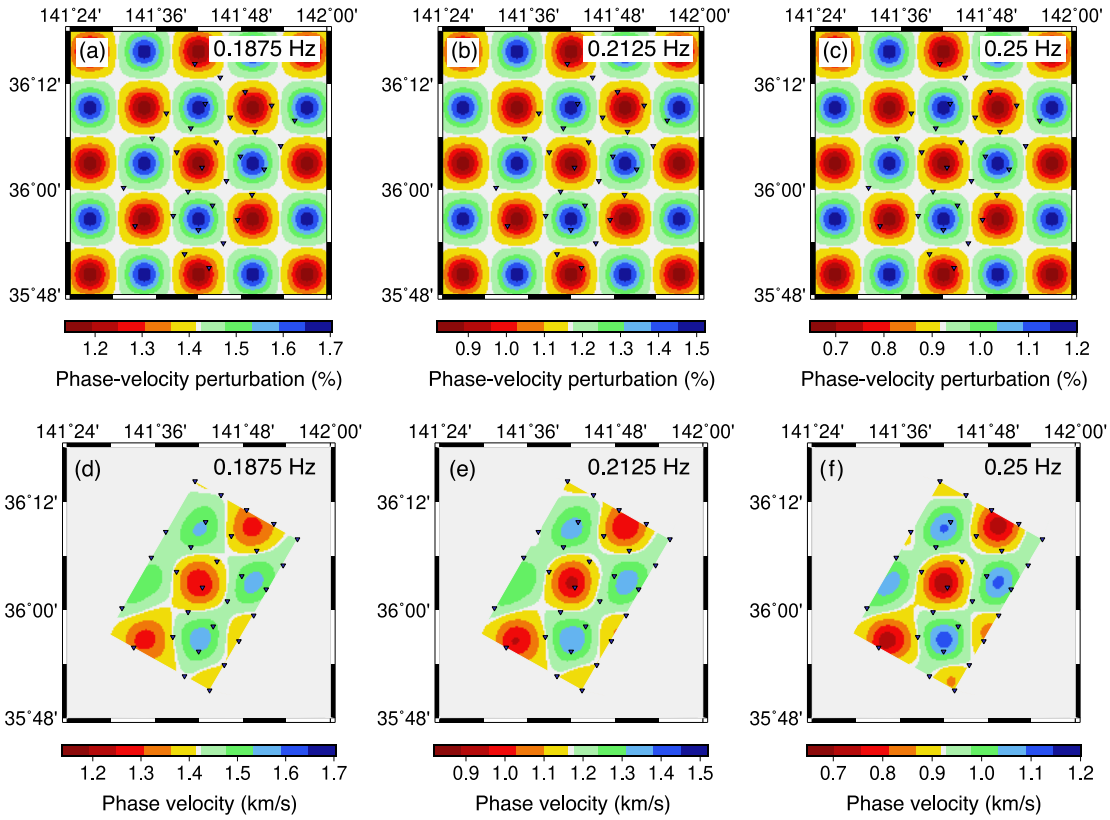

Figure S7. Checkerboard test for phase velocity distribution. (a–c) Input models for the first-higher mode of Rayleigh wave using the radial components. (d – f) Resulted models. (a, d) Input and resulted models using data obtained at 0.1875 Hz. (b, e) Models using data obtained at 0.2125 Hz. (c, f) Models using data obtained at 0.25 Hz.

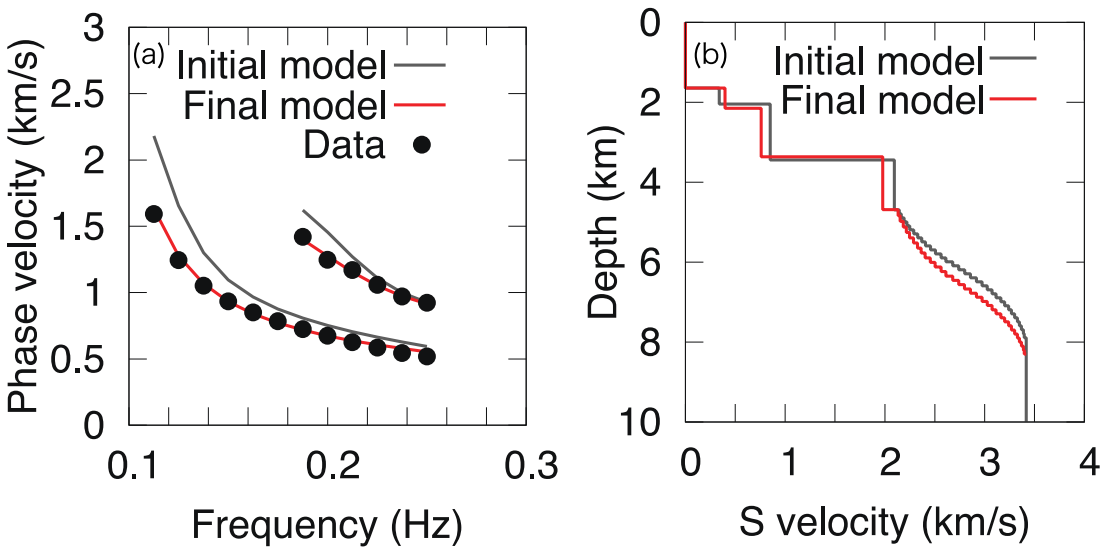

Figure S8. An example of local 1-D inversion. (a) Phase velocities for each frequency. Black dots show the phase velocities at a grid point. Grey curves show the dispersion curves of the reference 1-D model. Red curves show those of the final 1-D model at the grid point. (b) S-wave velocity models. Grey line shows the reference 1-D model and red line shows the final 1-D model, respectively.

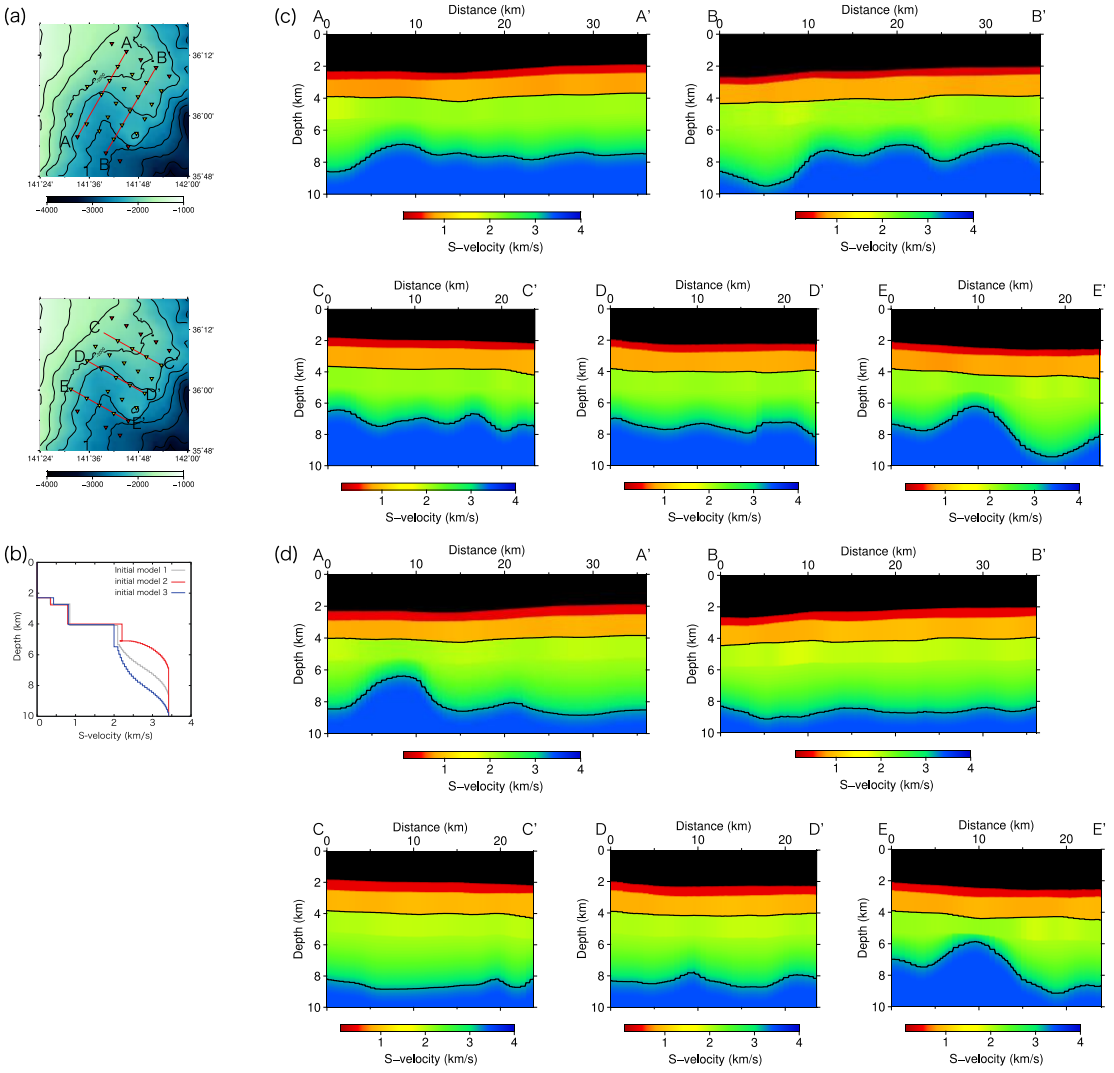

Figure S9. Cross-sections of 3-D S-wave velocity structure inferred from different initial models. (a) Locations of cross-sections. (b) Initial models. Initial model 1 is same as the initial model discussed in this study. Initial models 2 and 3 were used for checking the dependence of the final model on the initial models. (c) 3-D S-wave velocity model using initial model 2. (d) 3-D S-wave velocity model using initial model 3.

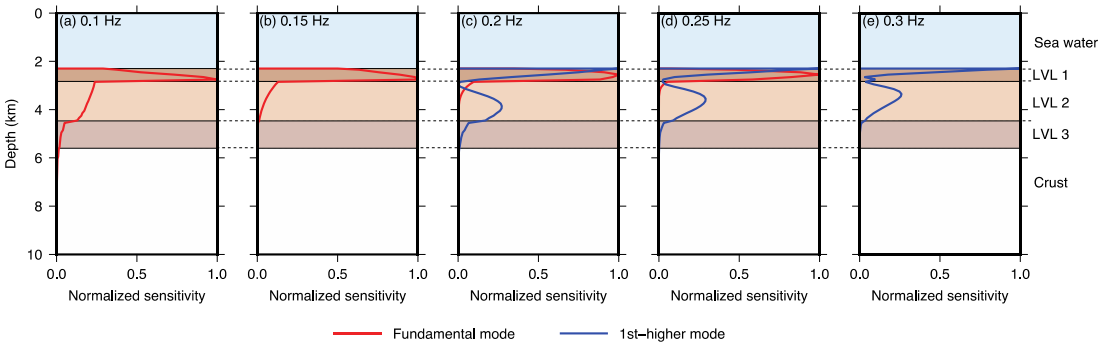

Figure S10. Sensitivity kernels of S-wave velocities for 0.1, 0.15, 0.2, 0.25, and 0.3 Hz. Red lines show the sensitivity kernels of the fundamental mode; blue lines show those of the first-higher mode.